GRSL-00616-2011

Hybrid Freeman/Eigenvalue Decomposition Method with Extended Volume Scattering Model

Gulab Singh, *Member, IEEE*, Yoshio Yamaguchi, *Fellow, IEEE*, Sang-Eun Park, *Member, IEEE*, Yi Cui, *Member, IEEE*, Hirokazu Kobayashi, Senior *Member, IEEE*,

***Abstract*— In this letter, an advanced version of the hybrid Freeman/eigenvalue decomposition technique for land parameters extraction is presented with an illustrative example of application. The motivation arises from decomposition problems in obtaining a meaningful volume scattering estimation, so that the technique can be used for both oriented objects and vegetation/forest areas. The idea is to improve the accuracy of the required parameter extraction. Two strategies are adopted to increase the applicability of a hybrid Freeman/eigenvalue technique: one is the unitary transformation of the coherency matrix; the other is to use an extended volume scattering model. The extension of the volume scattering model plays an essential role for the hybrid Freeman/eigenvalue technique. Since the volume scattering power is evaluated by assuming that the *HV* component is caused by vegetation only in the existing technique, an extended volume scattering power approach is utilized. It is shown that vegetation area and oriented objects such as urban building areas are well discriminated by the proposed technique as compared to the existing techniques.**

***Index Terms*— Hybrid Freeman/Eigenvalue Decomposition, POLSAR, unitary transformation, coherency matrix.**

I. INTRODUCTION

DECOMPOSITION of fully polarimetric data plays an important role in the interpretations, classifications and segmentations of POLSAR images, and in land parameter retrieval through inversion of decomposition images. Incoherent decomposition approaches (eigenvalue and model based decomposition approaches) are often applicable for classification and interpretation of POLSAR images [1]-[6]. Model based approaches are simple and straightforward to implement on fully polarimetric SAR data [2] - [5]. The three-component [3] and four-component decomposition [4], [5] schemes are well suited in that physical scattering models are used for typical targets classification and detection. Using these schemes, interpretations are easy and straightforward; however there is no guarantee of non-negative power occurrence. The solutions of the negative power problem were discussed by Van Zyl *et al.* [2] and Yajima *et al.* [4]. Van Zyl *et al.* [2] proposed a hybrid decomposition method to overcome negative power fatal deficiencies. Later, Arii *et al.* [6] extended the Van Zyl *et al.* [2] method to an adaptive model based decomposition method. Thereupon, Cloude [7] proposed a generalized hybrid Freeman/eigenvalue decomposition method for dealing with the negative power problems. The hybrid Freeman/eigenvalue decomposition is a mathematically and computationally very simple approach. The main idea of this approach is to use orthogonality to reduce the number of unknowns. In addition, the reformulation and computation of this approach enables a clearer study of the effectiveness of new scattering mechanism model.

On the other hand, the problem of overestimation of volume scattering power has been noticed from the azimuthally sloped surface and oblique urban blocks or man-made structures whose main scattering center is at an oblique direction with respect to radar illumination [5], [8]. The reason for this overestimation problem in the volume scattering power is that the polarization orientation shifts from the azimuthally sloped surface and oriented urban blocks or man-made structures with respect to radar illumination [5], [8]-[10], thus producing a higher cross-polarization (*HV*) intensity [11]. These effects in highly topographic surface regions can be reduced with the help of polarization orientation compensation or minimization of the cross-polarized component [8]-[11]. A method of rotation of the coherency matrix for minimizing its T_{33} element has been adopted to reduce the overestimation of the volume scattering component in oblique urban areas by Yamaguchi et. al. [5]. Later, it was pointed out that the idea of minimization of the T_{33} element is not sufficient for discriminating vegetation areas from oblique urban areas [12] since the volume scattering power is evaluated by the cross polarization component caused by vegetation only in the model based decomposition methods [3]-[5] and in the hybrid decomposition method [7]. As a result, the classification between vegetation and the buildings becomes difficult [12]. Therefore, we propose to use an extended volume scattering model [12] suited for oriented urban buildings (i.e., oriented dihedral model) to mitigate the overestimation problem. This proposed method shows the advancements in a 3-component hybrid decomposition scheme [7] for resolving the discrimination ambiguity of oriented dihedral objects from vegetation, by implementing the extended volume scattering model [12] and the concept of rotation about line of sight.

The brief description of the 3-component hybrid decomposition scheme [7] is described in Section II. The idea of rotation and unitary transformation of the coherency matrix is shown in Section III. Section IV provides the proposed scheme of 3-component hybrid decomposition for improving the results. Results of the proposed and existing hybrid

Manuscript received Oct. 14, 2011, revised Feb. 15, 2012 and March 19, 2012; accepted March 28, 2012. This work was supported by the grant of Space Sensing, Ministry of Education, Japan.

The authors are with Graduate School of Science and Technology, Niigata University, Japan. (phone/fax: +81-25-262-6752; e-mails: g.singh@ wave.ie.niigata-u.ac.jp; yamaguch@ ie.niigata-u.ac.jp).

decomposition schemes are compared and presented with illustrative examples in Section V. Furthermore, remarks on the hybrid decompositions are discussed in Section VI. Finally, in Section VII results of our new method are summarized.

II. Original 3-Component Hybrid Decomposition

This section explains briefly the hybrid Freeman/eigenvalue decomposition method [7] implementing the coherency matrix $[T]$ subject to the reflection symmetry condition. According to this hybrid scheme, $[T]$ is expanded into three sub matrices such as [7]

$$[T] = [T_S] + [T_D] + [T_V]$$

$$[T] = \begin{bmatrix} T_{11} & T_{12} & T_{13} \\ T_{21} & T_{22} & T_{23} \\ T_{31} & T_{32} & T_{33} \end{bmatrix},$$

$$[T_S] = m_s \begin{bmatrix} \cos^2\alpha_s & \sin\alpha_s \cos\alpha_s e^{j\phi_s} & 0 \\ \sin\alpha_s \cos\alpha_s e^{-j\phi_s} & \sin^2\alpha_s & 0 \\ 0 & 0 & 0 \end{bmatrix},$$

$$[T_D] = m_d \begin{bmatrix} \cos^2\alpha_d & \sin\alpha_d \cos\alpha_d e^{j\phi_d} & 0 \\ \sin\alpha_d \cos\alpha_d e^{-j\phi_d} & \sin^2\alpha_d & 0 \\ 0 & 0 & 0 \end{bmatrix},$$

$$[T_V] = m_v \begin{bmatrix} \frac{1}{2} & 0 & 0 \\ 0 & \frac{1}{4} & 0 \\ 0 & 0 & \frac{1}{4} \end{bmatrix} \quad (1)$$

In (1), $[T_S]$, $[T_D]$, and $[T_V]$ are the surface scattering, double bounce scattering and volume scattering matrices, respectively, and m_s, m_d, m_v are the corresponding, scattering power coefficients, respectively. $\alpha_s < \pi/4$ depends on the dielectric constant and angle of incidence and $\alpha_d > \pi/4$ depends on the angle of incidence and the two dielectric constants of surface and reflector. ϕ_s and ϕ_d are the scattering phase for surface and double bounce scattering, respectively. The key idea of orthogonality of the surface and dihedral component is applied in (1). The orthogonality condition can be expressed as [7]

$$\alpha_d + \alpha_s = \frac{\pi}{2}; \quad \text{with} \quad \phi_d - \phi_s = \pm\pi \quad (2).$$

Therefore, the orthogonality conditions reduce (α_d, α_s) to α, and (ϕ_d, ϕ_s) to ϕ in (1). Thus equation (1) is rewritten as

$$[T] = \begin{bmatrix} m_s \cos^2\alpha + m_d \sin^2\alpha & \cos\alpha \sin\alpha\, e^{j\phi}(m_d - m_s) & 0 \\ \cos\alpha \sin\alpha\, e^{-j\phi}(m_d - m_s) & m_d\cos^2\alpha + m_s\sin^2\alpha & 0 \\ 0 & 0 & 0 \end{bmatrix}$$

$$+ m_v \begin{bmatrix} \frac{1}{2} & 0 & 0 \\ 0 & \frac{1}{4} & 0 \\ 0 & 0 & \frac{1}{4} \end{bmatrix} \quad (3)$$

The scattering phase angle for dominant scattering mechanisms can be decided [7] based on the criteria in (4)

$$\phi = \begin{cases} \phi_s, \phi_d = 0 \;\; if \;\; \alpha \in [0, \pi/4] \;\; surface\; scattering \\ \phi_d, \phi_s = 0 \; if \; \alpha \in [\pi/4, \pi/2] \; dihedral\; scattering \end{cases} \quad (4)$$

The volume scattering component is derived as

$$m_v = 4T_{33} \quad (5)$$

This model can be inverted by calculating m_s and m_d as eigenvalues of the rank 2 matrix $[T_{SD}]$,

$$m_{d,s} = \frac{T_{11} + T_{22} - 3T_{33} \pm \sqrt{(T_{11} - T_{22} - T_{33})^2 + 4|T_{12}|^2}}{2} \quad (6)$$

III. Unitary Transformations Of Coherency Matrix

In this section, two (real and complex) unitary transformations are explained. First a real unitary transformation (RUT) of coherency matrix $[T]$ is introduced and is known as rotation of $[T]$ about the line of sight by angle θ in the literature [5], [11]. The coherency matrix can be defined for the compensation of polarization orientation shifts as

$$[T(\theta)] = \begin{bmatrix} 1 & 0 & 0 \\ 0 & \cos 2\theta & \sin 2\theta \\ 0 & -\sin 2\theta & \cos 2\theta \end{bmatrix} [T] \begin{bmatrix} 1 & 0 & 0 \\ 0 & \cos 2\theta & -\sin 2\theta \\ 0 & \sin 2\theta & \cos 2\theta \end{bmatrix} \quad (7)$$

where the rotation angle θ was derived in terms of coherency elements by Yamaguchi *et. al.* [5]. This rotation eliminates the real part of the element T_{23}. It is seen that T_{23} becomes pure imaginary. It can be noticed that after orientation compensation T_{23} is the best fit for the scattering helicity and roll-invariance [11].

The second unitary transformation is such that

$$T(\varphi) = [U(\varphi)][T(\theta)][U(\varphi)]^{\dagger}$$

$$= \begin{bmatrix} T_{11}(\varphi) & T_{12}(\varphi) & T_{13}(\varphi) \\ T_{21}(\varphi) & T_{22}(\varphi) & 0 \\ T_{31}(\varphi) & 0 & T_{33}(\varphi) \end{bmatrix} \quad (8)$$

with the unitary transform matrix,

$$[U(\varphi)] = \begin{bmatrix} 1 & 0 & 0 \\ 0 & \cos 2\varphi & j\sin 2\varphi \\ 0 & j\sin 2\varphi & \cos 2\varphi \end{bmatrix},$$

and $$2\varphi = \frac{1}{2}\, tan^{-1}\left(\frac{2\, Im\{T_{23}(\theta)\}}{T_{22}(\theta) - T_{33}(\theta)}\right) \quad (9)$$

This second complex unitary transformation will be treated as unitary change of basis matrix.

IV. 3-Component Hybrid Decomposition Method With Extended Volume Scattering Model

This section shows an improved methodology for the decomposition of fully polarimetric SAR data by using the real unitary transformation of the 3×3 coherency matrix (rotation of $[T]$ about the line of sight by angle θ [5]) and an extended volume scattering model [12]. This modification gives accurate or similar results in comparison to [7]. We expand the measured and rotated coherency matrix $[T(\theta)]$ under reflection symmetric scattering condition as,

$$[T(\theta)] = \begin{bmatrix} m_s \cos^2\alpha + m_d \sin^2\alpha & \cos\alpha \sin\alpha\, e^{j\phi}(m_d - m_s) & 0 \\ \cos\alpha \sin\alpha\; e^{-j\phi}(m_d - m_s) & m_d \cos^2\alpha + m_s \sin^2\alpha & 0 \\ 0 & 0 & 0 \end{bmatrix} + m_v \begin{bmatrix} F_s & F_{sd} & 0 \\ F_{ds} & F_d & 0 \\ 0 & 0 & F_v \end{bmatrix} \quad (10)$$

It should be remembered that the second unitary transformation (8) has not been applied in (10). However (8) can be applied in the decomposition scheme. Equation (8) does not change the properties of the volume scattering model as long as $[T_V]$ is developed under the assumption of azimuthal symmetric scattering with equal second and third diagonal elements [3]-[8], e.g., see $[T_V]$ in (1). Moreover, the second complex unitary transformation can be applied for accounting of the element T_{13} in [5] and guaranteeing the general applicability of the four component scattering power decomposition method [5] as will be discussed in Section VI.

The terms F_s, F_d, F_v, F_{sd} and F_{ds} are the elements of the volume scattering matrix. These elements of the volume scattering model are chosen, according to the generation of the cross-polarized *HV* term [12]. For volume scattering caused by the *HV* component by vegetation (dipole) (Re $\{S_{HH}\, S^*_{VV}\} \geq 0$), one of the following distributions is adopted based on the magnitude balance of $|S_{HH}|^2$ and $|S_{VV}|^2$, i.e., 1) uniform distribution, 2) cosine distribution, or 3) sin distribution from the reference [5]. For volume scattering caused by oriented dihedral scatter (Re $\{S_{HH}\, S^*_{VV}\} < 0$), we use the following probability distribution $p(\theta)$ with its peak centered on 0 degree [12]

$$p(\theta) = \frac{1}{2}\cos\theta \quad \text{for } -\frac{\pi}{2} < \theta < \frac{\pi}{2} \quad (11)$$

When these distributions are applied to the ensemble average of dipole scatterers or dihedral (horizontal or vertical) corner reflectors, the F_s, F_d, F_v, F_{sd} and F_{ds} elements can be determined. For example, based on (11), the following elements are obtained [12]

$$F_s = 0\,; F_d = \frac{7}{15}\,;\; F_v = \frac{8}{15}\,;\; F_{sd} = F_{ds} = 0 \quad (12).$$

By using (10) and (12), m_v is determined as

$$m_v = \frac{15}{8}\mathrm{T}_{33}(\theta) \quad (13)$$

The m_s and m_d can be calculated as eigenvalues of the rank 2 matrix $[T_{SD}]$ such as

$$m_{d,s} = \frac{\mathrm{T}_{11}(\theta) + \mathrm{T}_{22}(\theta) - (F_s + F_d)\, m_v}{2} \pm \frac{\sqrt{(\mathrm{T}_{11}(\theta) - \mathrm{T}_{22}(\theta) - (F_s - F_d) m_v)^2 + 4|(\mathrm{T}_{12}(\theta) - F_{sd}\, m_v)|^2}}{2} \quad (14)$$

It should be emphasized that highly accurate acquisition of the *HV* component with strong suppression of the noise floor is here of paramount relevance, and has been more or less totally overlooked in the past.

V. Results

The original and proposed decomposition schemes are applied to TerraSAR-X quad-polarization image data sets of April 21, 2010 over Niigata, Japan for verifying the correct implementation of the proposed scheme. For example, color-coded images over Niigata are displayed in Fig. 1. The window size for the ensemble average in image processing was chosen as 12 in the range direction and 10 in the azimuth direction which corresponds to 20 m by 20 m on the ground area. Results of the method derived in [7] are compared with the proposed method. Dynamic improvements of decomposition results are shown in Fig. 1. It is seen that the discrimination between the forest areas and agricultural areas is difficult in Fig. 1(c), whereas these two areas can be easily identified in Fig. 1 (b) by implementing the real rotation concept on the coherency matrix only. Whereas volume scattering in between forest areas and agricultural areas is separable by using the real rotation of coherency matrix, it was still difficult to discriminate agricultural areas from the oriented urban areas (Fig. 1 and Fig. 2) when based on the minimization of the T_{33} component only. This is because the *HV* component is assigned to the dipole scattering (volume scattering from vegetation) for generating Fig. 1(b) and (c). When the *HV* component is assigned to the dipole and dihedral scattering according to the extended volume scattering model in Fig. 1(a), in addition to the minimization of the T_{33} component, it is noticed that the double bounce scattering power P_d (Red) is either enhanced or kept similar in the proposed scheme (3-component hybrid decomposition + real rotation about line of sight + extension of volume scattering model) as compared to implementing the original 3-component hybrid decomposition with real rotation about line of sight or without real rotation about line of sight. This enhancement of Red in Fig. 1(a) as compared to Fig. 1(b) and 1(c) helps to resolve the discrimination ambiguity in between the man-made structures and vegetation areas. Close-up areas of a black rectangular box on Fig. 1 are shown in Fig. 2 to relate to the interesting observations of the double bounce scattering and the volume scattering appraisal over the oriented urban areas. The

improvements are clearly seen in the determination of the double bounce scattering and the volume scattering by the proposed scheme over the oriented urban area and the intermittent and surrounding vegetated environments. Results are confirmed using Google optical images that are shown in Fig. 2(a). Fig. 2 (b) shows good discrimination in between dihedral and other scatterers as compared to Figs 2 (c) and 2(d). The green color of the oriented urban area is suppressed in Fig. 2(b) as compared to Fig. 2(c) and 2(d).Vegetation areas are displayed similarly in both images (Fig. 2(b) and 2(c)).

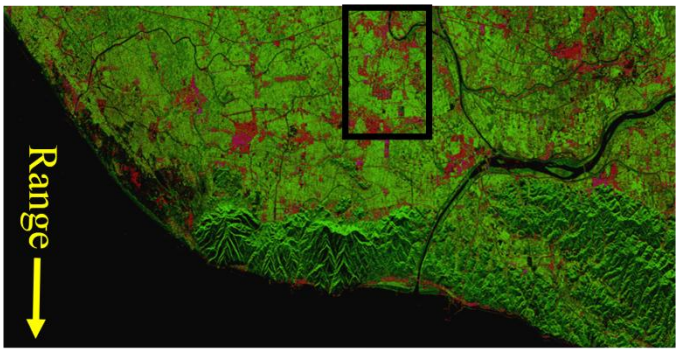

(a)

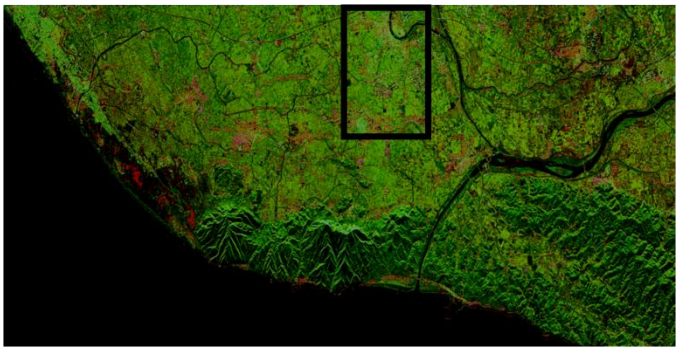

(b)

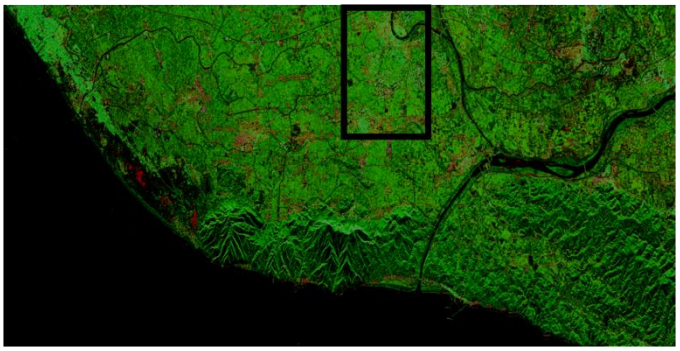

(c)

Fig. 1. Color-coded decomposition image with Red (m_d: double bounce), Green (m_v: volume scattering), Blue (m_s: surface scattering) (a) new hybrid decomposition with rotation about line of sight (real unitary transformation only) and extended volume scattering model (b) original hybrid decomposition with rotation about line of sight (real unitary transformation only) (c) original hybrid decomposition

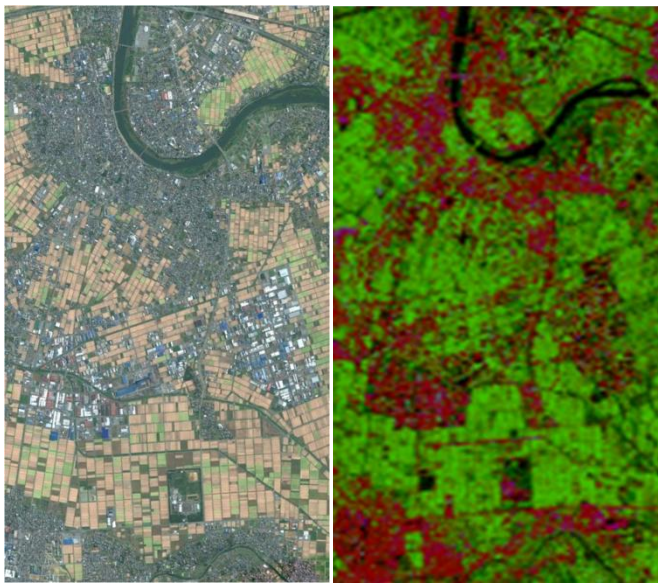

(a) (b)

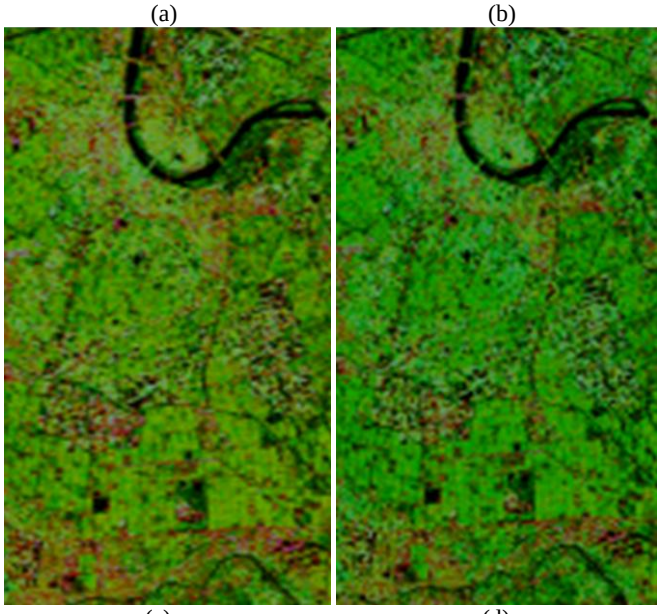

(c) (d)

Fig. 2. Close-up areas of black box areas on Fig. 1, color-coded decomposition image with Red (m_d: double bounce), Green (m_v: volume scattering), Blue (m_s: surface scattering): (a) Google optical image (b) new hybrid decomposition with rotation about line of sight and extended volume scattering model (c) original hybrid decomposition with rotation about line of sight (d) original hybrid decomposition.

VI. Remarks and Future Work

In general, the results of the new hybrid decomposition scheme are remarkable for the case of the reflection symmetric condition but results over highly oriented urban areas are not satisfactory. Since the 3-component hybrid method works under the reflection symmetry assumption, this assumption causes an over-estimation problem in volume scattering power in highly oriented urban areas and for sloped terrain [5]. However, an outstanding approach of Arii *et. al.* [6] accounts for all polarimetric measurements and becomes a generalized

4-component hybrid-model-based decomposition scheme under the non-reflection symmetry condition. The Arii *et. al.* [6] decomposition forces the third eigenvalue (known as remainder in their approach) of $[T_{SD}]$ to be minimized. It may be possible that the remainder in [6] can be further minimized by extracting the helix scattering power at the initial stage of the decomposition scheme when the coherency matrix $[T_{SD}]$ holds for the non-reflection symmetry condition with existence of the helical scattering component (in highly oriented urban areas and for sloped terrain). Moreover, a generalized volume scattering model with non-reflection symmetry assumption was applied, while surface scattering and double bounce scattering coherent models were considered under reflection symmetry [6]. Our interest is to explore the consideration of the aforementioned issues in future work and to understand the effect of reflection symmetric depolarization (incoherent surface and double bounce scattering models) on results after inclusion in the decomposition schemes. On other hand, by applying the second unitary transformation of the coherency matrix, it may be possible to use all 7 elements of the unitary transformed coherency matrix $[T(\varphi)]$ without the reflection symmetry assumption in the linear fitting model based 4-component scattering powers decomposition method [5] such as

$$T(\varphi) = m_s[U(\varphi)][T_s][U(\varphi)]^{\dagger} + m_d[U(\varphi)][T_D][U(\varphi)]^{\dagger} + m_v[U(\varphi)][T_V][U(\varphi)]^{\dagger} + m_c[U(\varphi)]\begin{bmatrix}0 & 0 & 0\\ 0 & 1 & \pm j\\ 0 & \mp j & 1\end{bmatrix}[U(\varphi)]^{\dagger} \quad (15)$$

Furthermore, to understand the depolarization (in incoherent surface $[T_S]$ and double bounce $[T_D]$ scattering models) effects on the decomposition behavior, the extended surface and double bounce scattering models can be adopted in (15) from [7] and [13]. In (15), the extended volume scattering model $[T_V]$ can be used similar to that of (10).

VII. Summary and Conclusion

An improved hybrid decomposition scheme is presented in this letter. The resultant decomposition image is as good as compared to [7]. However, the overall results of the improved hybrid decomposition scheme are good enough subject to relying on the reflection symmetric condition but results over highly oriented inclined regions are not reasonable, and are mixed with contributions from vegetation areas. In addition, an alternative procedure was proposed to account for the reflection symmetric depolarization and full polarimetric information in decomposition. In the near future, the effects of reflection symmetric depolarization and accounting for full polarimetric information in the decomposition schemes will be analyzed in more detail.

Acknowledgment

The authors are grateful to DLR for providing the desired fully polarimetric Quad-Pol TerraSAR-X data sets, respectively. The authors would like to thank Prof. W.-M. Boerner, Professor Emeritus at the University of Illinois at Chicago to suggesting improvements for the manuscript.

References

[1] R. Touzi, "Target scattering decomposition in terms of roll-invariant target parameters," *IEEE Trans. Geosci. Remote Sens.*, vol. 45, pp. 73-84, Jan. 2007.

[2] J. J. van Zyl, M. Arii, and Y. Kim, "Requirements for Model-Based Polarimetric Decompositions," *Proc. of IGARSS08*, Boston, MA, Jul. 2008.

[3] A. Freeman and S. Durden, "A three-component scattering model for polarimetric SAR data," *IEEE Trans. Geosci. Remote Sens.*, vol. 36, no. 3, pp. 963-973, May 1998.

[4] Yajima, Y. Yamaguchi, R. Sato, H. Yamada, and W.-M. Boerner, "POLSAR image analysis of wetlands using a modified four-component scattering power decomposition," *IEEE Trans. Geosci. Remote Sens.*, vol. 46, no. 6, pp. 1667-1773, June 2008.

[5] Y. Yamaguchi, A. Sato, W.-M. Boerner, R. Sato, and H. Yamada, "Four-component scattering power decomposition with rotation of coherency matrix," *IEEE Trans. Geosci. Remote Sens.*, vol. 49, no. 7, pp. 2251-2258, July 2011.

[6] M. Arii, J. J. van Zyl, and Y. J. Kim, "Adaptive model-based decomposition of polarimetric SAR covariance matrices," *IEEE Trans. Geosci. Remote Sens.*, vol. 49, no. 3, pp. 1104 – 1113, Mar. 2011.

[7] S. R. Cloude, *Polarisation: Applications in Remote Sensing*. London,U.K.: Oxford Univ. Press, 2009.

[8] J. S. Lee, D.L. Schuler, and T.L. Ainsworth, Polarimetric SAR data compensation for terrain azimuth slope variation, *IEEE Trans. Geosci. Remote Sens.*, vol. 38, no. 5, pp. 2153-2163, Sept. 2000.

[9] J. S. Lee, D.L. Schuler, T.L. Ainsworth, E. Krogager, D. Kasilingam, and W. M. Boerner, On the estimation of radar polarization orientation shifts induced by terrain slopes, *IEEE Trans. Geosci. Remote Sens.*, vol. 40, no.1, pp. 30 41, Jan. 2002.

[10] F. Xu, and Y. Q. Jin, "Deorientation theory of polarimetric scattering targets and application to terrain surface classification," *IEEE Trans. Geosci. Remote Sens.*, vol. 43, no. 10, pp. 2351-2364, Oct. 2005.

[11] J. S. Lee and T. Ainsworth, "The effect of orientation angle compensation on coherency matrix and polarimetric target decompositions," *IEEE Trans. Geosci. Remote Sens.*, vol. 49, no. 1, pp. 53-64, Jan. 2011.

[12] A. Sato, Yoshio Yamaguchi, G. Singh, and S.-E. Park,"4-component scattering power decomposition with extended volume scattering model", *IEEE Geosci. Remote Sens. Lett.*, vol. 9, no. 2, pp. 166 – 170, Mar. 2012.

[13] J. S. Lee, T.L. Ainsworth and Y. Wang, "Recent advances in scattering model-based decompositions: An overview", *Proc. of IGARSS11*, Vancouver, Canada, Jul. 2011.